

## Intergranular Giant Magnetoresistance in a Spontaneously Phase Separated Perovskite Oxide

J. Wu,<sup>1</sup> J. W. Lynn,<sup>2</sup> C. J. Glinka,<sup>2</sup> J. Burley,<sup>3</sup> H. Zheng,<sup>3</sup> J. F. Mitchell,<sup>3</sup> and C. Leighton<sup>1,\*</sup>

<sup>1</sup>Department of Chemical Engineering and Materials Science, University of Minnesota, Minneapolis, Minnesota 55455, USA

<sup>2</sup>NIST Center for Neutron Research, National Institute of Standards and Technology, Gaithersburg, Maryland 20899, USA

<sup>3</sup>Materials Science Division, Argonne National Laboratory, Argonne, Illinois 60439, USA

(Received 9 July 2004; published 25 January 2005)

We present small-angle neutron scattering data proving that, on the insulating side of the metal-insulator transition, the doped perovskite cobaltite  $\text{La}_{1-x}\text{Sr}_x\text{CoO}_3$  phase separates into ferromagnetic metallic clusters embedded in a nonferromagnetic matrix. This induces a hysteretic magnetoresistance, with temperature and field dependence characteristic of intergranular giant magnetoresistance (GMR). We argue that this system is a natural analog to the artificial structures fabricated by depositing nanoscale ferromagnetic particles in a metallic or insulating matrix; i.e., this material displays a GMR effect without the deliberate introduction of chemical interfaces.

DOI: 10.1103/PhysRevLett.94.037201

PACS numbers: 75.47.De, 75.47.Gk, 85.75.-d

The colossal magnetoresistance (CMR) in perovskite oxides [1,2], and the giant magnetoresistance (GMR) in metallic heterostructures [3–5] have revolutionized our understanding of correlated electron physics and spin transport in heterogeneous solids. Although they seemingly originate from very different physics (GMR is observed in artificial heterostructures, CMR in bulk materials), recent progress has led to the realization that heterogeneity also plays a key role in understanding CMR [6]. The essential concept is that these randomly doped oxides exhibit spatial coexistence of ferromagnetic (F) metallic regions and non-F insulating regions [6–9]. Doped cobaltites such as  $\text{La}_{1-x}\text{Sr}_x\text{CoO}_3$  have been shown to exhibit a particularly clear form of this inhomogeneity by electron microscopy [10] and nuclear magnetic resonance (NMR) [11–13]. The phase separation occurs in addition to the well-known spin-state transitions arising from the comparable sizes of the Hund rule exchange energy and crystal field splitting [14]. Co NMR [11] reveals the coexistence of F metallic, low spin insulating, and glassy non-F regions at all  $x$ , although the F phase dominates for  $x > 0.18$ . The metal-insulator transition (MIT) at  $x = 0.18$  and the coincident F ordering are then interpreted as percolation of isolated F regions [15,16].

We present here small-angle neutron scattering (SANS) *proving* that in the insulating phase of  $\text{La}_{1-x}\text{Sr}_x\text{CoO}_3$ , i.e.,  $x < 0.18$ , nanoscale F clusters form in a non-F matrix. Combining these data with single crystal magnetotransport we find that the formation of F clusters leads to the onset of a previously unobserved hysteretic GMR-type effect with field and temperature dependencies correlated with the cluster sizes and populations. This behavior is reminiscent of artificially heterostructured materials composed of F clusters deposited in a non-magnetic metallic [17,18] or insulating [19–23] matrix. We argue that the phase inhomogeneity in this perovskite leads to the natural formation of a granular ferromagnet-semiconductor system, analogous to the artificial granular systems used to investigate GMR,

but without the deliberate introduction of chemical interfaces.

Absolute SANS measurements were done at a wavelength of  $5 \text{ \AA}$ , at  $0.01 < q < 0.30 \text{ \AA}^{-1}$ , using  $10 \mu\text{m}$  grain size polycrystals fabricated by solid-state reaction [15]. We focused on three representative compositions:  $x = 0.15$  (in the semiconducting “spin-glass phase”),  $x = 0.18$  (the critical composition for cluster percolation), and  $x = 0.30$  (in the F phase) [15,16]. In order to investigate intrinsic transport we also grew floating zone single crystals of  $\text{La}_{1-x}\text{Sr}_x\text{CoO}_3$  ( $0.00 < x < 0.20$ ), which were found single phase by neutron and x-ray diffraction.

An example of the  $q$  dependence of the SANS is shown in Fig. 1(a), for  $x = 0.3$ , i.e., well into the F metallic phase, where the Curie temperature,  $T_C$ , is 220 K. Strong magnetic scattering is observed, with the low  $q$  intensity increasing rapidly below  $T_C$ . This magnetic low  $q$  scattering follows the well-known Porod form,  $I(q) = 6\pi(\Delta d)^2/Rq^4$  (dotted line, Fig. 1), where  $R$  is the radius of the scattering centers and  $\Delta d$  is the scattering length density contrast. This results from a 3D distribution of “hard spheres” in the regime  $q \gg R^{-1}$  and is often observed in Fs due to scattering from domains [24–26]. Observation of this form down to  $q = 0.01 \text{ \AA}^{-1}$  directly implies that this  $x = 0.3$  sample exhibits long-range (length scales  $\gg 2\pi/0.01 \text{ \AA}^{-1} \approx 600 \text{ \AA}$ ) F order. At  $T > T_C$ ,  $I(q)$  consists of weak scattering from the grains, which was minimized by employing large grain size polycrystals (as opposed to previous work on powder [27]). Near  $T_C$  significant intensity is observed at high  $q$ , following the Lorentzian form,  $I(q) = I_0/(q^2 + \kappa^2)$ , with  $I_0$  and  $\kappa$  constants. This has been observed in many F materials [24,28] and is due to the quasielastic critical scattering near  $T_C$ . The quantity  $\kappa = 1/\xi$ , where  $\xi$ , the correlation length, diverges as  $T \rightarrow T_C$  [24,28].

Examining Fig. 1 it is clear that the intensity can be separated into low  $q$  scattering (due to long-range ordered F domains) and higher  $q$  Lorentzian scattering (due to short-range fluctuations). We therefore present the  $T$  dependence of the two types simply by plotting the low  $q$

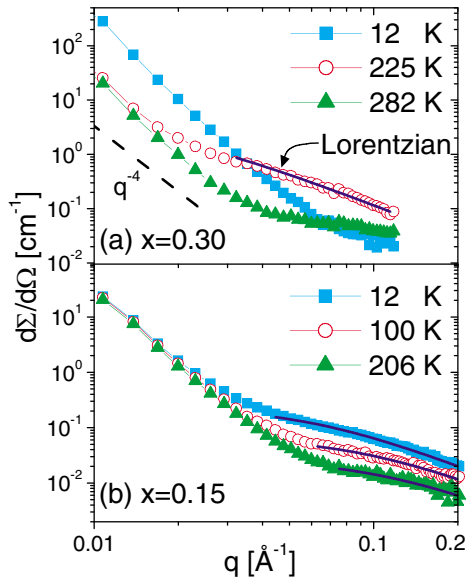


FIG. 1 (color online).  $q$  dependence of the absolute SANS intensity for (a)  $x = 0.30$  at  $T = 12, 225,$  and  $282$  K, and (b)  $x = 0.15$  at  $T = 12, 100,$  and  $206$  K. The dashed line shows the Porod form [ $I(q) \sim q^{-4}$ ] and the solid lines are fits to the Lorentzian functional form.

intensity [ $I(q = 0.01 \text{ \AA}^{-1})$ ] (Fig. 2, top panel) and the high  $q$  intensity [ $I(q = 0.06 \text{ \AA}^{-1})$ ] (Fig. 2, middle panel), along with the  $T$  dependence of the magnetization,  $M$ , from conventional magnetometry (bottom panel). Starting at  $x = 0.30$ , which we have already shown to be a long-range ordered F (consistent with neutron diffraction [10,27]), we find a sharp increase in the low  $q$  intensity at  $T_C$ , in agreement with  $M(T)$ . The corresponding high  $q$  data show a narrow peak [full width at half maximum (FWHM)  $\approx 30$  K] near  $T_C$ , due to the expected critical scattering. For  $x = 0.18$ , i.e., the critical composition separating long-range F order and metallicity from glassy magnetism and

semiconducting behavior, the situation is different. The low  $q$  scattering is less intense and has a broad onset near  $T_C$ , whereas the high  $q$  scattering exhibits a wide peak (FWHM  $\approx 80$  K), reflecting the fact that long-range order is barely stable. At  $x = 0.15$  the low  $q$  intensity is weak, with no discernible transition to long-range F order. Despite this, the magnetization at low  $T$  is almost 25% of that observed at  $x = 0.30$ , i.e., deep in the F phase. The origin of this magnetization is clarified by the high  $q$  intensity which shows a  $T$  dependence that closely mimics  $M(T)$ , in stark contrast to  $x = 0.18$  and  $0.30$ . Given that this high  $q$  scattering is due to short length-scale F correlations it is clear the large magnetization at  $x = 0.15$  results from F clusters that have not yet coalesced.

The Lorentzian form allows for a simple extraction of the magnetic correlation length,  $\xi$  (Fig. 3). At  $x = 0.30$  the spin correlations form above  $T_C$  and  $\xi$  diverges as  $T_C$  is approached due to the onset of long-range order. For  $x = 0.18$ , however, the correlation length, although it increases near “ $T_C$ ,” does not diverge. This composition is at the boundary between short- and long-range ordering and does not have a well-defined  $T_C$ . For  $x = 0.15$  the Lorentzian form is still observed at high  $q$  [Fig. 1(b)], but no critical divergence exists due to the absence of a transition to long-range order. Instead,  $\xi$  increases below  $150$  K [Fig. 3(c)], due to nucleation of isolated F clusters, which eventually attain correlation lengths  $\sim 15\text{--}25 \text{ \AA}$  at low  $T$ . Although we cannot clearly differentiate between purely electronic phase separation and inhomogeneities due to local variations in composition, we note that there is no signature of chemical clustering in the SANS.

The picture that emerges at  $x = 0.15$  is of isolated F clusters embedded in a non-F matrix. In order to correlate the information provided by SANS about the population and sizes of these clusters with the electronic properties, we examined magnetotransport in single crystals near the

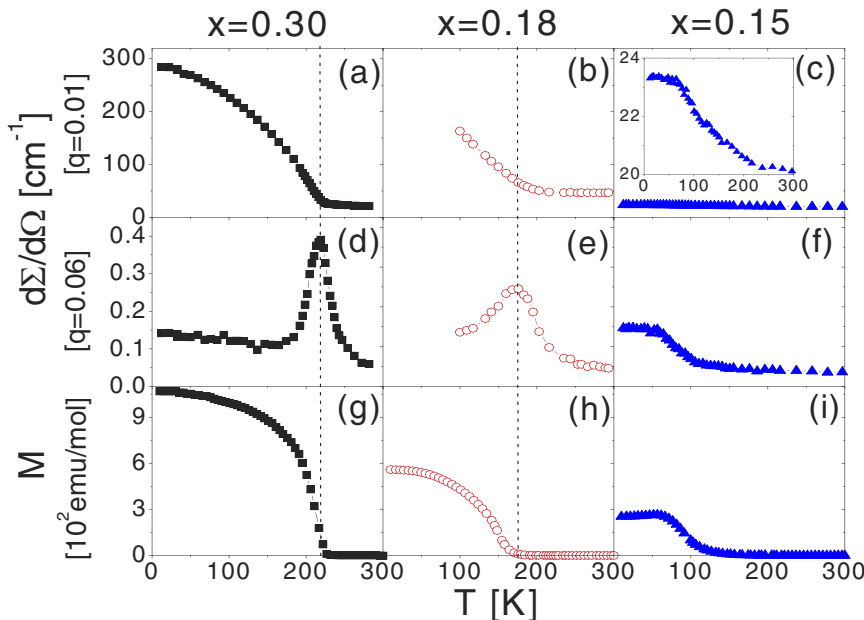


FIG. 2 (color online).  $T$  dependence of the SANS intensity at low  $q$  (top panel), high  $q$  (middle panel), and the field cooled (10 Oe)  $M(T)$  (bottom panel). Data are shown for  $x = 0.30$  (left panel),  $x = 0.18$  (center panel), and  $x = 0.15$  (right panel). The inset to (c) is simply the data of (c) on an expanded scale.

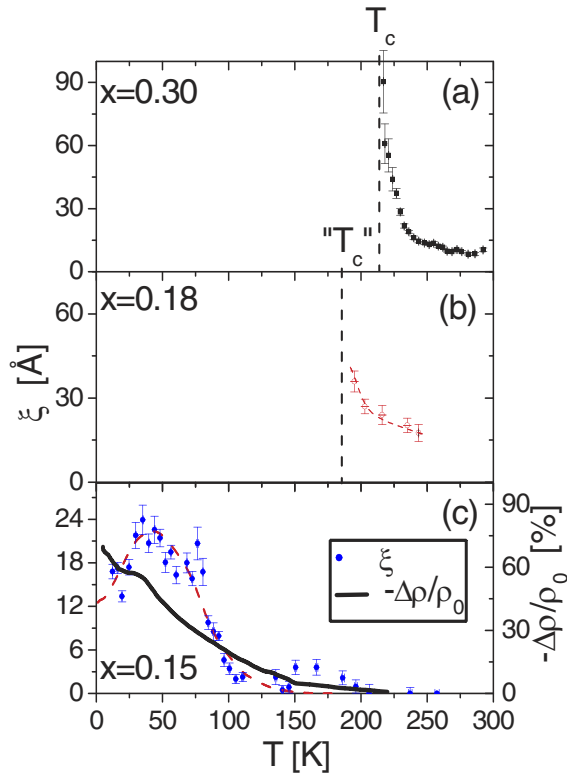


FIG. 3 (color online).  $T$  dependence of the magnetic correlation length,  $\xi$ , for (a)  $x = 0.30$ , (b)  $x = 0.18$ , and (c)  $x = 0.15$ . The thick solid line in (c) shows the 90 kOe MR for  $x = 0.15$  (right axis). The dashed lines are guides to the eye.

MIT. The  $T$  dependence of the resistivity ( $\rho$ ) for  $0.00 < x < 0.20$  is shown in Fig. 4. At  $x \geq 0.17$  we find positive values of  $d\rho/dT$  at high  $T$  and a finite  $T = 0$  conductivity, indicating metallic behavior. Typical nonhysteretic negative MR ( $\sim 20\%$ ) is observed in the vicinity of  $T_C$  for the metallic samples. The MR on the insulating side of the MIT is of more interest and is shown in Fig. 5 for  $x = 0.15$  at  $T = 10$  K. Large negative MR is observed  $\{[\rho(H) - \rho(0)]/\rho(0) = -68\%$ , which persists to high field, is hysteretic, and exhibits distinct differences between the virgin curve and subsequent field cycles (see the detail near  $H = 0$ ).  $\rho(H)$  displays peaks at  $H = \pm 6.5$  kOe, which corresponds closely with the coercive field ( $H_C$ ) extracted from  $M(H)$  (6.4 kOe). This effect occurs only at low  $T$ , as shown in Fig. 3(c), which plots the  $T$  dependence of the 90 kOe MR. The MR becomes evident at the same temperature as the first indications of cluster nucleation, meaning that the hysteretic MR occurs only when F clusters form in the semiconducting non-F matrix. This point is further reinforced by the inset to Fig. 5, which shows the composition dependence. The MR decreases rapidly at the MIT, where the isolated F clusters cease to exist due to their coalescence into a percolated network. Moreover, as is also shown in this figure, the MR has distinctive hysteresis, with resistivity peaks at  $H_C$ , for all of the insulating compositions ( $x < 0.17$ ), but this hysteresis disappears at higher doping (solid points denote hysteretic MR while

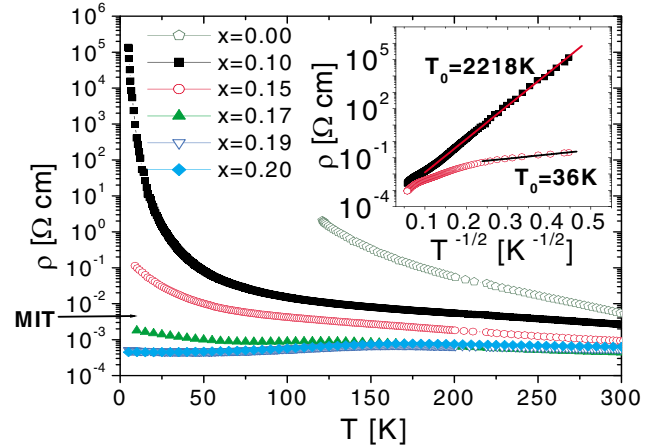


FIG. 4 (color online).  $T$  dependence of the resistivity for six single crystals ( $0.00 < x < 0.20$ ). Inset:  $T$  dependence of the resistivity at  $x = 0.10$  and  $0.15$  plotted as  $\rho$  (log<sub>10</sub> scale) vs  $T^{-1/2}$ . The solid lines are straight line fits resulting in  $T_0 = 2218$  and  $36$  K, respectively.

open points indicate no hysteresis). Note that this MR is not due to spin-dependent tunneling between grains, as seen in polycrystalline CMR materials [2,29], as our specimens are single crystal.

These qualitative features exhibit remarkable similarity to the negative intergranular MR previously observed in artificial structures composed of nanoscale F particles in an insulating or metallic nonmagnetic matrix. The insulating matrix systems Co-SiO<sub>2</sub> [22,23] and Ni-SiO<sub>2</sub> [19–21] have been studied since the 1970s while interest in metallic matrix systems such as Co-Cu [17,18] and Fe-Cu [17] was stimulated by the discovery of GMR in 1986 [3]. These systems are fabricated by cosputtering and are composed of 10–70 Å F clusters embedded in a non-F matrix

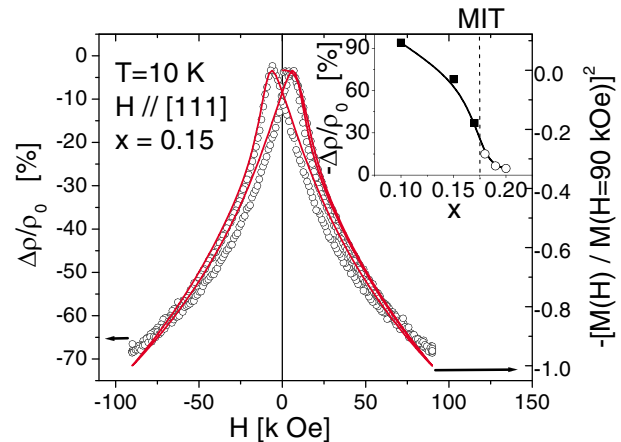


FIG. 5 (color online). 10 K magnetoresistance of an  $x = 0.15$  single crystal measured with  $H$  parallel to [111] and perpendicular to the sample plane (and current), after zero field cooling. Open symbols correspond to the MR (left axis), while the solid line corresponds to  $M(H)$  (right axis). Inset: doping dependence of the MR. Solid points represent hysteretic MR and the open symbols indicate no hysteresis.

[18,19,21–23]. The insulating matrix systems display sizable MR [22], with noticeable differences between the virgin curve and subsequent cycles [22], as well as an MR that decreases rapidly beyond percolation. The metallic matrix systems have GMR up to  $-23\%$  at 5 K in a 50 kOe field [18], a nonsaturating response to 50 kOe [17], and strong hysteresis [17,18]. Quite simply, we suggest that  $\text{La}_{1-x}\text{Sr}_x\text{CoO}_3$  is a naturally occurring analog of these artificial granular systems, as all of the features observed in the low  $T$  MR are consistent with those seen in the artificial granular materials. In our case the system spontaneously phase separates into metallic F clusters of diameter  $\sim 25$  Å embedded in a semiconducting matrix of hole-poor non-F material. The heterogeneity is therefore provided by the spontaneous magnetoelectronic phase inhomogeneity as opposed to artificial heterostructuring. The hysteretic low  $T$  MR then arises due to spin-dependent transport between F clusters. The resistivity is maximized at  $\pm H_C$  (where  $M = 0$ ) and is reduced in applied fields due to alignment of the cluster magnetizations [30]. Considering the semiconducting nature of our matrix it is unsurprising that the  $\text{La}_{1-x}\text{Sr}_x\text{CoO}_3$  MR displays features consistent with both the insulating and metallic matrix systems. Note that in our case the matrix is itself magnetic (albeit non-F) meaning that a high field response is expected due to polarization of the matrix.

These qualitative statements can be strengthened by two quantitative analyses. In the artificial matrix systems the MR scales with  $M$  as  $[\rho(H) - \rho(H_C)]/\rho(H_C) \propto -[M(H)/M_S]^2$  [17,22], where  $M_S$  is the saturation magnetization [31]. The agreement with this scaling form (both on the virgin curve and subsequent cycles) is shown in Fig. 5, where the solid line depicts the square of the experimental  $M/M_S$ . (Note that a similar scaling applied to manganites [1] was developed for the nonhysteretic CMR near  $T_C$  and models completely different physics.) It has also been shown that in the insulating matrix systems  $\rho(T)$  follows  $\rho = \rho_0 \exp(T_0/T)^{1/2}$ , with  $\rho_0$  and  $T_0$  constants [20,22]. This occurs due to tunneling or hopping between clusters in the presence of a Coulomb energy penalty for charging the clusters [20] (or possibly a more complex mechanism [20]) and is quite distinct from Efros-Shklovskii variable range hopping [32], despite the identical  $\rho(T)$ . Such a  $T$  dependence is indeed observed in the insulating phase, as shown in the inset to Fig. 4. At  $x = 0.10$  the  $T^{-1/2}$  form is observed over 2 orders of magnitude in  $T$  with  $T_0 = 2200$  K, similar to the Co, Ni-SiO<sub>2</sub> systems [19–23], where  $T_0$  is in the range 182–4500 K. At  $x = 0.15$ , closer to the MIT, the adherence to  $T^{-1/2}$  is less convincing, although there may be an approach to this form at low  $T$ .

In summary, we have presented small-angle neutron scattering and magnetotransport showing that the spontaneously phase separated perovskite oxide  $\text{La}_{1-x}\text{Sr}_x\text{CoO}_3$  is the first known natural analog to artificial structures composed of ferromagnetic particles embedded in nonferromagnetic insulating or metallic matrices. This allows us to

observe an intergranular GMR effect without the deliberate introduction of chemical interfaces.

We gratefully acknowledge use of neutron facilities at NIST. Work at ANL was supported by U.S. DOE under W-31-109-ENG-38. Instrumentation (UMN) was supported by NSF MRSEC (DMR-0212302). We acknowledge discussions with I. Terry, S. Giblin, and B. I. Shklovskii.

\*Corresponding author.

Electronic address: leighton@umn.edu

- [1] Y. Tokura and Y. Tomioka, *J. Magn. Magn. Mater.* **200**, 1 (1999).
- [2] J. M. D. Coey *et al.*, *Adv. Phys.* **48**, 167 (1999).
- [3] M. N. Baibich *et al.*, *Phys. Rev. Lett.* **61**, 2472 (1986).
- [4] I. K. Schuller *et al.*, *J. Magn. Magn. Mater.* **200**, 571 (1999).
- [5] J. Bass and W. P. Pratt, Jr., *J. Magn. Magn. Mater.* **200**, 274 (1999).
- [6] E. Dagotto *et al.*, *Phys. Rep.* **344**, 1 (2001).
- [7] M. Fath *et al.*, *Science* **285**, 1540 (1999).
- [8] Ch. Renner *et al.*, *Nature (London)* **416**, 518 (2002).
- [9] M. Hennion *et al.*, *Phys. Rev. Lett.* **81**, 1957 (1998).
- [10] R. Caciuffo *et al.*, *Phys. Rev. B* **59**, 1068 (1999); J. Mira *et al.*, *J. Appl. Phys.* **89**, 5606 (2001).
- [11] P. L. Kuhns *et al.*, *Phys. Rev. Lett.* **91**, 127202 (2003); M. J. R. Hoch *et al.*, *Phys. Rev. B* **69**, 014425 (2004).
- [12] A. Ghoshray *et al.*, *Phys. Rev. B* **69**, 064424 (2004).
- [13] W. G. Moulton *et al.* (to be published).
- [14] For a short review, see M. Imada *et al.*, *Rev. Mod. Phys.* **70**, 1039 (1998) (in particular, refer to pp. 1235–1239).
- [15] J. Wu and C. Leighton, *Phys. Rev. B* **67**, 174408 (2003).
- [16] M. A. Senaris-Rodriguez and J. B. Goodenough, *J. Solid State Chem.* **118**, 323 (1995).
- [17] J. Q. Xiao *et al.*, *Phys. Rev. Lett.* **68**, 3749 (1992).
- [18] A. E. Berkowitz *et al.*, *Phys. Rev. Lett.* **68**, 3745 (1992).
- [19] J. I. Gittleman *et al.*, *Phys. Rev. B* **5**, 3609 (1972).
- [20] P. Sheng *et al.*, *Phys. Rev. Lett.* **31**, 44 (1973); M. Pollak and C. J. Adkins, *Philos. Mag. B* **65**, 855 (1992); J. Zhang and B. I. Shklovskii, *Phys. Rev. B* **70**, 115317 (2004).
- [21] J. S. Helman and B. Abeles, *Phys. Rev. Lett.* **37**, 1429 (1976).
- [22] S. Barzilai *et al.*, *Phys. Rev. B* **23**, 1809 (1981).
- [23] S. Sankar *et al.*, *J. Magn. Magn. Mater.* **221**, 1 (2000); S. Sankar *et al.*, *Phys. Rev. B* **62**, 14273 (2000).
- [24] J. W. Lynn *et al.*, *Phys. Rev. Lett.* **80**, 4582 (1998).
- [25] C. Yaicle *et al.*, *Phys. Rev. B* **68**, 224412 (2003).
- [26] Ch. Simon *et al.*, *Phys. Rev. Lett.* **89**, 207202 (2002).
- [27] R. Caciuffo *et al.*, *Europhys. Lett.* **45**, 399 (1999).
- [28] J. W. Lynn *et al.*, *Phys. Rev. Lett.* **76**, 4046 (1996); J. M. de Teresa *et al.*, *Nature (London)* **386**, 256 (1997).
- [29] S. Lee *et al.*, *Phys. Rev. Lett.* **82**, 4508 (1999).
- [30] The relative magnitude of the resistivities in the virgin and coercive states provides information on interdot magnetic correlations [23]. Equal magnitudes in our case suggest that these correlations are weak.
- [31] In the absence of saturation in  $M(H)$  [15] we simply normalized to the 9 T value.
- [32] B. I. Shklovskii and A. L. Efros, *Electronic Properties of Doped Semiconductors* (Springer-Verlag, New York, 1984).